Weak decay of ^{130}Ba and ^{132}Ba: Geochemical measurements

A. P. Meshik,[1] C. M. Hohenberg,[1] O. V. Pravdivtseva,[1] and Ya. S. Kapusta[2]

[1]*Physics Department, Washington University, St. Louis, Missouri 63130*
[2]*Activation Laboratories, Ancaster, Ontario, Canada L9G 4V5*

The half-life of ^{130}Ba due to multichannel weak decay ($2\beta^+$, 2EC, and ECβ^+) has been determined for the first time by the measurement of the ^{130}Xe daughter accumulated in natural barite (BaSO$_4$) from the Belorechenskoe deposit in North Caucasus, Russia. The accumulation time was determined from U-Xe and K-Ar gas-retention ages measured in the same material, yielding a half-life for ^{130}Ba for all weak decay modes of $2.2 \pm 0.5 \times 10^{21}$ yr (68% C.L.), about a factor of 2 lower than that predicted by the proton-neutron quasiparticle random phase approximation. From excess ^{132}Xe observed in this barite, the half-life for weak decay of ^{132}Ba can be estimated ($T_{1/2} = 1.3 \pm 0.9 \times 10^{21}$ yr). However, this value is more tentative, since other sources of this isotope cannot be excluded, but the lower limit of 2.2×10^{21} yr remains firm.

INTRODUCTION

Double positron emission and double electron capture ($2\beta^+$, β^+EC, 2EC) are the lesser investigated channels of electroweak decay compared with conventional double beta decay $2\beta^-$. Contributing factors are generally low Q values (decay energies) for the $2\beta^+$, β^+EC, and 2EC channels and long predicted half-lives, especially for the $2\beta^+$ transition [1,2]. However, the pertinent nuclear matrix elements are not very well constrained and do not seem to have predictable trends [2], leading to considerable uncertainty. The case is less dismal for 2EC transitions to excited states [3,4]; it may be possible to detect these decay modes using geochemical accumulation methods which are more sensitive than direct counting experiments.

Determination of decay constants by geochemical methods is based upon the accumulation of daughter products in minerals of known age. The most favorable cases occur when the daughter products are isotopes of xenon and, to a less extent, krypton, where the low natural abundances and the large number of stable isotopes permit resolution of small radiogenic contributions. This technique was first applied to the investigation of the $2\beta^-$ decay of ^{130}Te in 1950 by Inghram and Reynolds [5]. Since that time, the half-life of this transition has been measured and refined by many different laboratories [6–18]. The sensitivity and precision of the geochemical method are amply demonstrated in the determination of the $2\beta^-$ decay half-life of ^{128}Te (to ^{128}Xe). At $7.7 \pm 0.4 \times 10^{24}$ yr, this is the longest half-life ever measured experimentally [17,18]. Geochemically determined 2β-decay rates of the shorter-lived ^{82}Se [16] are in excellent agreement with those determined by direct counting methods [19,20].

If any of the electroweak decay modes of ^{130}Ba have half-lives of 10^{22} yr or less, it may be possible to detect the ^{130}Xe daughter product in the Xe spectrum of geologically old Ba-rich mineral deposits. From proton-neutron quasiparticle random phase approximations (pn-QRPAs), the half-lives for the $2\beta^+$, β^+EC, and 2EC decay modes of ^{130}Ba are predicted to be about 1.7×10^{29}, 1.0×10^{23}, and 4.2×10^{21} yr, respectively [4]. While the first two ($2\beta^+$ and β^+EC) half-lives look hopelessly long for measurement by either geochemical or direct counting methods, the double K-capture (2EC) mode might be accessible geochemically. However, the pn-QRPA calculations, extended by the multiple communicator model (MCM) [2], suggest a half-life of 4.7×10^{23} yr for 2EC ^{130}Ba decay, well above the experimental detection limit. Detection of ^{130}Ba decay in geologically old samples can test the validity of these different theoretical models as well as provide measurement of its half-life.

So far, the only known search for ^{130}Xe from ^{130}Ba was reported by Srinivasan [20] who measured Xe in old barites (BaSO$_4$) from South Africa and Australia. In that work, however, the presence of other Xe components (spallation from high-energy cosmic-ray interactions, neutron captures on various Ba isotopes, and ^{238}U fission) prevented resolution of any contribution from weak decay. Later, Barabash and Saakyan [3] reexamined the data of Srinivasan and, making various assumptions, estimated a lower limit for the half-life of ^{130}Ba at $T_{1/2} > 4 \times 10^{21}$ yr. The work reported here represents a new attempt to measure the half-life of ^{130}Ba using refined analytical methods and samples carefully selected to reduce interferences. The particular barite chosen for this study has negligible contributions from spallation, n capture, and the $\beta\beta^-$ decay of ^{130}Te, making it more suitable than the material analyzed in the earlier studies.

SAMPLE SELECTION

Although barium in the Earth's crust is a much more abundant element than tellurium, it is much more difficult to detect weak decays of ^{130}Ba than the $\beta\beta^-$ decay of ^{130}Te. First, it is difficult to find stable, high-purity, Ba-rich minerals of documented age, suitable for the geochemical investigation of Ba electroweak decay (most barium minerals are affected by hydrothermal processes). Second, the isotopic abundance of ^{130}Ba(0.106%) is much lower than that of ^{130}Te(33.87%) and Ba is present in minerals most abundantly as BaSO$_4$ whereas Te is often found as the pure native metal. This implies that, in order to detect a similar half-lives with Ba and Te samples of the same antiquity, it would take 500 times more barite than native tellurium. This means that interferences and background of trapped atmospheric xenon, which are both normally proportional to sample mass, will

be much higher in the barite experiment, making it much more difficult to detect small additions of a radiogenic daughter than in the tellurium experiment. Considering the long theoretical half-life predictions (pn-QRPA) for the electroweak decay of ^{130}Ba [2,4], measurement will be difficult, even for geologically old samples. Solving this problem will require substantial amounts of material and careful analytical technique. Although it is not a problem to locate kilogram quantities of pure barite, it is not easy to make a low-blank high-vacuum oven for such large samples. The blank problem is further exacerbated by the mineral itself. BaSO$_4$ decomposes upon heating in vacuum, releasing large quantities of highly reactive SO$_2$. This gas attacks the sample system, releasing significant quantities of Xe from the interior surfaces. As a compromise, $\sim$5 g of BaSO$_4$ was chosen as the optimum sample size for this study. Even this required four stages of chemical gettering and careful data analysis.

Five "promising" barites were initially selected from a variety of sites. In order to minimize contributions from cosmic-ray spallation reactions, the most desirable samples should come from a large enough depth that cosmic-ray effects are suitably attenuated. All candidate samples were recovered from depths of at least 100 m, had low concentrations of uranium and thorium, and had well-documented geological histories. Atmospheric Xe, present in all barites, is a background that can be subtracted since its isotopic composition is known [29]. However, in order to measure small contributions from weak decay, it is necessary to minimize contributions from other sources that are not so well characterized. To determine the best among these five samples, Xe isotopic compositions were measured in small ($<$0.1 g) aliquots from each. Four of them had clear signatures of spallation-produced Xe, indicating near-surface residence some time in their geologic history. The presence of ^{131}Xe excesses (from neutron capture on ^{130}Ba) in three of the barites indicates significant exposure to epithermal neutrons compared with the other two samples, an effect which is commonly observed in barites [20,21], but which complicates the analysis for low-level isotopic effects.

One of the five samples was clearly superior to the others. It contained relatively small amounts of indigenous Xe, atmospheric in composition, accompanied by minor contributions from other sources, providing a background most suitable for the detection of low-level ^{130}Xe additions from the weak decay of ^{130}Ba. That sample, from the Belorechenskoe barite deposit, Northern Caucasus, Russia [22], was selected for the more detailed experimental procedures. This hydrothermal deposit was formed in successive stages, with quartz-dolomite, ankerite, and barite-calcite veins, intersecting fault dislocations and surrounded by Lower and Middle Paleozoic formations with more recent granite intrusions [23]. Dolomite veins post-date the host rock and provide a reference geologic age of $1.70 \pm 0.15 \times 10^8$ yr (beginning of the Middle Jurassic) [25]. Both dolomite and barite are secondary minerals, but the dolomite veins are crossed by barite veins, establishing this age as an upper limit for the age of the barite. Our particular sample was of the third morphological type, forming at 105–110 °C [24], a nearly pure BaSO$_4$ of tabular structure, with SrO being the major impu-

rity [0.31 wt %, determined using inductively coupled plasma (ICP) mass spectrometry]. Although the relatively young age of this sample must be considered a disadvantage, many older hydrothermal barites show evidence of internal metasomatism (i.e., they were redeposited during late-stage or post-formation hydrothermal activity). In the Belorechenskoe sample, the barite veins show no evidence for hydrothermal activity since formation.

EXPERIMENT

The isotopic composition of xenon from 60 mg of Belorechenskoe barite in the initial preliminary examination was indistinguishable from that of atmospheric Xe. Once this sample was selected, a more detailed analysis would be required to separate the atmospheric component, to identify any other components present, and to resolve Ba-derived ^{130}Xe. For this, we selected two additional samples to study using stepwise extraction techniques in two different gas-handling systems. Both of these samples were pre-degassed at $\sim$150 °C in vacuum to remove superficial atmospheric contamination.

The first stepwise extraction was performed using 0.4234 g barite in a small tungsten coil, a procedure originally designed for subgram-sized samples where extremely low blanks were required [26]. The coil temperature was originally calibrated against the input power using an optical pyrometer, but as a result of the open coil design, the sample temperature is substantially lower than that of the coil. BaSO$_4$ decomposes at 900–1100 °C in vacuum, releasing Xe from its lattice. We were not able to melt the more refractory BaO, which remained in the coil, by raising the temperature further. Although the higher-temperature fractions did release considerable amounts of Xe (due to chemical reaction of the SO$_2$ decomposition product with interior surfaces of the sample system), they were atmospheric in composition with very little additional contributions of radiogenic ^{130}Xe or ^{238}U fission Xe.

The second stepwise heating experiment was done with a single 3.783-g piece of the Belorechenskoe barite in an oven of special design for low blanks with larger sample size [27]. This oven uses separate vacuums for the sample and the tantalum resistance heater, and an embedded W-W/Re thermocouple for temperature control. Procedural blanks run at 1000 °C, accumulated for 30 min, were $\sim$5$\times$10^{-14} cm^3 STP of ^{132}Xe, $\sim$50 times higher than those of the small oven, but 10 times lower than the smallest temperature fraction of Xe released from the barite. The Belorechenskoe barite was the first sample analyzed in this oven, eliminating the possibility of memory effects. Xe from this larger sample was extracted in five temperature steps of 700, 900, 1100, 1480, and 1700 °C, each maintained for 30 min. The gases released at each temperature were purified from chemically active species in four sequential stages of gettering (three successive steps to SEAS-type 707 getter pellets and to a freshly deposited titanium film). Light noble gases were removed from the Xe by selective desorption from activated charcoal. The purified Xe was then admitted and analyzed statically in a 20-cm magnetic sector ion-counting mass spectrometer [26]

TABLE I. Concentrations and isotopic compositions of xenon (^{132}Xe$\equiv$100) measured in Belorechenskoe barite in two different stepwise heating experiments. Temperatures for the first run are estimates; the uncertainties shown are 1σ (68% C.L.). ''Subtotal'' corresponds to Xe released at temperatures of 1000 °C and below. ''Total'' includes Xe from all temperatures (see text).

T (°C)	^{132}Xe (10^{-11} cm^3 STP/g)	^{124}Xe	^{126}Xe	^{128}Xe	^{129}Xe	^{130}Xe	^{131}Xe	^{134}Xe	^{136}Xe
	First run, 0.4234 g, extraction in small low blank oven								
~800	0.2489	0.3735	0.3326	7.105	98.70	15.301	79.184	38.828	33.180
	±0.0011	±0.0075	±0.0083	±0.044	±0.32	±0.076	±0.219	±0.154	±0.116
~1100	0.4067	0.3615	0.3268	7.164	98.21	15.197	78.829	38.978	33.338
	±0.0012	±0.0048	±0.0065	±0.035	±0.24	±0.057	±0.160	±0.098	±0.100
Subtotal	0.6956	0.3660	0.3290	7.141	98.40	15.236	78.964	38.921	33.278
	±0.0016	±0.0041	±0.0051	±0.027	±0.19	±0.046	±0.129	±0.085	±0.076
~1500	0.1083	0.3674	0.3475	7.129	98.24	15.309	78.545	38.781	32.973
	±0.0008	±0.0229	±0.0118	±0.095	±0.44	±0.107	±0.305	±0.224	±0.205
Total	0.7639	0.3662	0.3316	7.140	98.37	15.247	78.904	38.901	33.235
	±0.0018	±0.0048	±0.0047	±0.027	±0.18	±0.042	±0.119	±0.079	±0.072
	Second run, 3.7830 g, extraction in high-capacity double vacuum oven								
700	0.0851	0.3538	0.3276	7.098	97.74	15.132	78.596	39.023	33.241
	±0.0003	±0.0032	±0.0029	±0.018	±0.13	±0.023	±0.076	±0.057	±0.054
900	0.164	0.3537	0.3309	7.103	97.63	15.281	78.628	38.931	33.273
	±0.001	±0.0036	±0.0033	±0.022	±0.14	±0.032	±0.093	±0.111	±0.058
1100	0.0136	0.3440	0.3174	6.911	96.54	14.874	77.431	39.270	33.640
	±0.0001	±0.0175	±0.0122	±0.095	±0.74	±0.144	±0.677	±0.435	±0.308
Subtotal	0.2625	0.3532	0.3291	7.092	97.61	15.212	78.556	38.978	33.282
	±0.0035	±0.0026	±0.0024	±0.016	±0.11	±0.023	±0.072	±0.075	±0.043
1480	0.782	0.3514	0.3304	7.106	98.09	15.069	78.762	38.747	32.974
	±0.001	±0.0040	±0.0036	±0.046	±0.46	±0.057	±0.352	±0.176	±0.129
1710	1.648	0.3559	0.3306	7.116	97.99	15.085	78.729	38.740	32.885
	±0.001	±0.0025	±0.0027	±0.016	±0.12	±0.022	±0.076	±0.060	±0.032
Total	2.693	0.3544	0.3304	7.110	97.98	15.093	78.721	38.765	32.949
	±0.004	±0.0019	±0.0020	±0.017	±0.15	±0.022	±0.112	±0.063	±0.049
	Reference xenon isotope compositions								
Atmospheric Xe [29]		0.3536	0.33077	7.0989	98.112	15.1290	78.9055	38.7819	32.916
		±0.0012	±0.00072	±0.0029	±0.041	±0.0047	±0.0076	±0.0069	±0.017
Xe from ^{238}U fission [30,31]		0	0	0	<0.3	0	14.63	142.2	172.1
							±0.34	±0.4	±0.9

whose sensitivity and mass discrimination (~0.02% per amu) were determined before and after each sample with Xe calibration spikes.

In order to measure potassium (for K-Ar dating) and uranium (for U-Xe dating), barite aliquots of about 0.2 g were weighed and placed into a pure graphite crucible along with a standard flux to facilitate melting (~1.2 g of lithium metaborate, lithium tetraboraye, and lithium carbonate). The sample was fused in a Leco furnace and the potassium content determined using optical emission spectrometry ICP-OES (Thermo Jarrell Ash Enviro II) calibrated with three international standards. The ^{238}U content was measured by ICP mass spectrometry (Perkin Elmer ELAN 6000) calibrated with suitable uranium standards.

RESULTS AND DISCUSSION

The melting point of barite at atmospheric pressure is reported to be 1580 °C. However, as suspected from the analysis of the stepwise heating data and confirmed by off-line experiments, BaSO$_4$ decomposes into SO$_2$, BaO, and oxygen when heated in vacuum. In the temperature range 900–1100 °C, the BaSO$_4$ visibly changed from a blocky white crystalline form to a fine powder, releasing SO$_2$, which was detected by reaction with a copper test foil. Subsequent analyses, using the energy-dispersive x-ray analysis (EDX) mode of the JEOL-840A scanning electron microscope, confirmed the presence of sulfur compounds on the test foil. The highly reactive SO$_2$ degrades surfaces of the sample system, releasing adsorbed atmospheric Xe. While this compromises
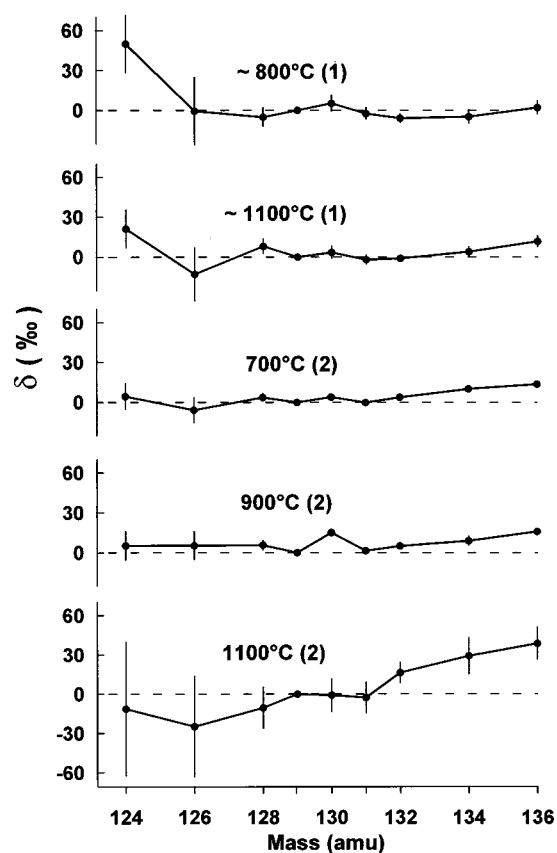
FIG. 1. Permil deviation of the Xe isotopic composition from atmospheric Xe, normalized to ^{129}Xe (run numbers in parentheses). Temperature fractions above 1100 °C are not shown since they are dominated by spurious atmospheric Xe (see text) and plot as horizontal lines. Most temperature fractions demonstrate slight enrichments at ^{130}Xe and the heavy isotopes (fission), most precisely shown in 900 °C of the second run.

the usefulness of the higher-temperature fractions, by the time this occurs most of the radiogenic ^{130}Xe has already been released.

The quantity and isotopic composition of Xe released during two stepwise extractions of the Belorechenskoe barite are shown in Table I and plotted in Fig. 1 as permil deviations from atmospheric Xe composition. The temperature fractions above 1100 °C are dominated by extraneous atmospheric Xe released by the chemical reaction of SO_2 and are not shown. If we ignore a minor ($<2\sigma$) ^{124}Xe excess in the first run, there is no indication of spallation-produced enrichment of the low-abundance light Xe isotopes (where such effects would be most evident). This indicates substantially complete shielding from galactic cosmic rays, distinguishing this sample from that of the earlier study of Srinivasan [20] and assuring that the ^{130}Xe will have no spallation component. Contributions from the spontaneous fission of ^{238}U are present at the heavy neutron-rich isotopes. These, along with the measured radiogenic ^{40}Ar, play a vital role in constraining the gas retention age of this sample. ^{129}Xe has one of the highest abundances in atmospheric Xe and a low yield in ^{238}U fission ($<0.012\%$ compared to 6% for ^{136}Xe [28]).

Consequently, ^{129}Xe is the preferred tracer for atmospheric Xe and is used as the reference isotope in δ plots of Fig. 1. Xe from any additional nuclear process will manifest itself as a positive δ value (note that no negative δ values are observed). Any isotopic fractionation of the atmospheric component would be indicated by sloped lines in Fig. 1, with both positive and negative δ values; none is observed. Although the presence of a small amount of fractionation has little impact on the measured ^{130}Xe excesses (^{129}Xe, the reference isotope, is adjacent to ^{130}Xe), it is more important in determining the quantity of fission Xe, as will be addressed below. As previously mentioned, reaction of SO_2 in the higher-temperature fractions releases additional atmospheric Xe (Table I), diluting the visibility of the Ba-derived Xe for the *bulk* sample. However, in the 700 and 900 °C fractions in the second run and, to a lesser extent, in the 800 and 1100 °C in the first run, there are clear excesses of ^{130}Xe, coupled with fission-produced Xe from ^{238}U. Since ^{130}Xe is shielded by stable ^{130}Te in fission, it can only be the product of ^{130}Ba decay. The correlation between radiogenic ^{130}Xe and fission Xe is important for two reasons. First, resolution of the fission component provides a means to measure the Xe retention age of the sample (essential for determination of the ^{130}Ba half-life). More important, though, this release confirms the temperature of vacuum decomposition of $BaSO_4$, that point at which radiogenic ^{130}Xe accumulated from the weak decay of ^{130}Ba will be released. To summarize, predegassing of the sample at several hundred degrees in vacuum removes much of the superficial atmospheric Xe; stepwise heating allows the two radiogenic components (^{130}Xe and fission Xe) to be resolved in the 700–1100 °C fractions from additional atmospheric Xe released at the higher temperatures.

In order to determine the amount of radiogenic ^{130}Xe present in the barite, trapped Xe must first be removed. While it is clear from the delta plots shown in Fig. 1 that this trapped Xe, traced by the quantity of ^{129}Xe, is very nearly atmospheric in composition, a small amount of mass fractionation may still be present. To detect any linear mass fractionation of trapped atmospheric Xe, a series of spectral decompositions was made using a range of mass fractionations. Removing the known ^{238}U fission Xe composition and a correctly fractionated atmospheric Xe should leave zero residuals at all isotopes except ^{130}Xe from ^{130}Ba decay. To determine the specific mass fractionation which best fits the data, the sum of the weighted square residuals of all Xe isotopes was minimized, excluding ^{131}Xe (which can have neutron capture contributions [21]) and ^{132}Xe (which may have contributions from ^{132}Ba weak decay). The best fit was found for a slightly negative mass fractionation of -0.05% per amu. While allowing for a small degree of mass fractionation has only a small effect on the quantity of radiogenic ^{130}Xe derived compared with unfractionated atmospheric Xe (less than 5%), it has a somewhat larger effect on the quantity of fission Xe (30%) and consequently on the implied U-Xe age.

The amount of radiogenic ^{130}Xe is found by subtracting the slightly fractionated atmospheric Xe from each of the individual temperature fractions, assigning all of the ^{129}Xe to

that source. This leaves only fission Xe and radiogenic ^{130}Xe (Fig. 2). As can be seen, the residuals are zero within error for all other isotopes except for an enrichment at ^{132}Xe, which, although small ($<2\sigma$), may be due to the weak decay of ^{132}Ba. Summing the contributions in the temperature fractions 1100 °C and below ("subtotal," Table I), we obtain the following values for the radiogenic ^{130}Xe:

$(4.6\pm3.6)\times10^{-15}$ cm^3 STP ^{130}Xe/g for the first run,

$(4.36\pm1.03)\times10^{-15}$ cm^3 STP ^{130}Xe/g

for the second run,

and similarly for the concentrations of ^{238}U fission Xe:

^{136}Xe$_f=(2.15\pm0.62)\times10^{-14}$ cm^3 STP/g in the first run,

^{136}Xe$_f=(1.69\pm0.14)$

$\times10^{-14}$ cm^3 STP/g in the second run.

Remarkably, while the precision of the data and the concentrations of *trapped* Xe in two runs are quite different, the calculated radiogenic ^{130}Xe and ^{238}U fission Xe concentrations are essentially the same for these two runs. Inclusion of the higher-temperature fractions (which contain spurious Xe of atmospheric composition released by SO$_2$ reaction) has a negligible effect on the measured quantities of either the radiogenic ^{130}Xe or the fission xenon, but it increases the uncertainties since more atmospheric Xe is subtracted. Moreover, once the barite lattice is disrupted, release of *in situ*–produced radiogenic components is complete. We can combine these two measurements as weighted means to obtain final values (radiogenic ^{130}Xe$=4.38\pm0.99$ $\times10^{-15}$ cm^3 STP/g, fissiogenic ^{136}Xe$=1.72\pm0.14$ $\times10^{-14}$ cm^3 STP/g), but the results are clearly dominated by the greater precision of the second run.

An additional potential interference must be carefully considered before concluding that all of the radiogenic ^{130}Xe is due to decay of ^{130}Ba. As mentioned earlier, ^{130}Te is more effective than ^{130}Ba in producing ^{130}Xe by $\beta\beta$ decay (greater abundance and comparable half-life) and the presence of only 1% Te can produce the observed ^{130}Xe excesses. Evaluation of this possibility requires assessment of the Te concentration in this sample. Although difficult to do by either ICP mass spectrometry or neutron activation analysis due to formidable interferences in both techniques, there are other nonchemical methods at our disposal sensitive enough to set appropriate upper limits. Using the EDX mode of the JEOL-840A scanning electron microscope, we examined the tellurium L line (3.769 keV) and found no Te signal above the detection limit. In order to calibrate the Te L-line sensitivity and determine its detection limit, we prepared a series of Te-Au standards with Te contents of 1%, 0.1%, 0.05%, and 0.01%. Metallic tellurium was weighted with a CAHN C-31 microbalance, added to a predetermined quantity of gold, and fused. After melting, the resulting pellets were cut up, remixed, and melted again to achieve a uniform Te distribution. To verify, x-ray spectra were taken from several differ-

ent areas of each sample, confirming Te homogeneity to within 5%. Clear Te signals were obtained for all but the most dilute standard, establishing the Te detection limit at <0.05 wt % Te. This implies that Te would have been detected in the barite if it had been present at the 0.05% level where it would contribute less than 5% of the observed radiogenic ^{130}Xe. Therefore, more than 95% of the excess ^{130}Xe must be due to ^{130}Ba.

Once the quantity of ^{130}Ba-derived ^{130}Xe is established, its half-life can be found using the gas-retention age of the sample. This must be equal to or lower than the $1.70\pm0.15\times10^8$ yr age of the dolomite veins in the host rock [15]. The gas-retention age of the barite itself, however, can be determined using U-Xe and K-Ar ages measured in the actual sample. Since all of the daughter products are noble gases, fissiogenic Xe, the ^{40}Ar from potassium decay, and the ^{130}Xe from ^{130}Ba should have accumulated for the same length of time. The potassium content (0.020 ± 0.003 wt %) and the concentration of radiogenic argon ^{40}Ar ($9.8\pm0.7\times10^{-8}$ cm^3/g) measured in this sample provide a bulk K-Ar age of $1.24\pm0.22\times10^8$ yr. The ^{238}U content (0.235 ± 0.025 ppm) and the measured concentration of ^{136}Xe from ^{238}U fission ($1.72\pm0.14\times10^{-14}$ cm^3 STP/g) sample likewise provide a U-Xe retention age of $1.43\pm0.23\times10^8$ yr, using the two most recent measurements of ^{238}U fission production rates [17,18]. Since the K-Ar and U-Xe ages are totally independent of each other and concordant within the stated uncertainties, the gas-retention age for the Belorech-
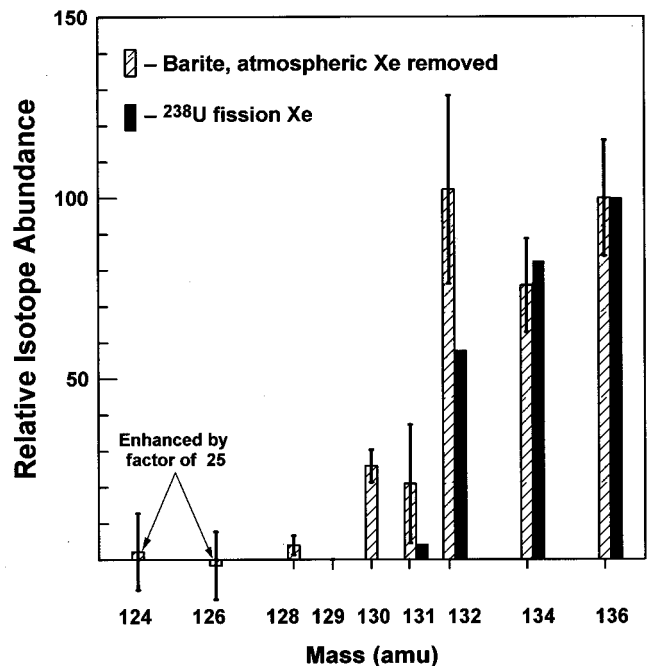

FIG. 2. Xe from Belorechenskoe barite (second run) after subtraction of fractionated (-0.05% amu) atmospheric Xe. The vertical scale has been increased by a factor of 25 at mass 124 and 126. Radiogenic ^{130}Xe and ^{238}U fission Xe are most evident, with a small excess (less than 2σ) at ^{132}Xe, suggestive of double beta decay of ^{132}Ba. Excess ^{131}Xe from neutron capture on ^{130}Ba is quite small (1σ).

enskoe barite is confidently taken as the average of these two values: $1.34 \pm 0.12 \times 10^8$ yr. This postdates (by about 25%) the reported geologic age of the dolomite in the host rock, as expected since the barite is typically hydrothermal in origin and observed in secondary veins that transect the dolomite [25].

From the measured radiogenic ^{130}Xe and the gas-retention age of this barite, the ^{130}Ba half-life is found to be $2.16 \pm 0.52 \times 10^{21}$ yr. This electroweak multichannel half-life is about 2 times lower than that predicted by pn-QRPA [4], not bad as these things go. Since the 2EC decay channel of ^{130}Ba probably has the shortest half-life of the three available channels [1], this value probably pertains to the double K-capture channel.

The small residual excess ^{132}Xe (less than 2σ), observed in Fig. 2, may be due to the double beta decay of ^{132}Ba, but the case for this is less certain than for ^{130}Ba. The difficulty is due to the isotopic abundance of ^{132}Xe being 6 times greater in atmospheric Xe than ^{130}Xe, and 98% of the ^{132}Xe in this barite is atmospheric in origin. Therefore, the excess ^{132}Xe shown in Fig. 2 is much more dependent on mass fractionation (e.g., the uncertainty of this excess goes from about 40% for -0.05%/amu mass fractionation to 63% for no fractionation). In addition, the effective ^{132}Xe (and the ^{131}Xe) yield in ^{238}U fission can be modified by chemical migration, especially if carried by fluids [32]. While the apparent excess ^{132}Xe in Fig. 2 can be used to estimate the half-life of ^{132}Ba weak decay ($T_{1/2} = 1.3 \pm 0.9 \times 10^{21}$ yr), other sources of ^{132}Xe cannot easily be excluded. It is, therefore, less certain than the ^{130}Ba half-life, but the value of 2.2×10^{21} yr is a rigid lower limit and almost an order of magnitude larger than the previous lower limit for the weak decay half-life of ^{132}Ba [3].

[1] J. Suhonen and O. Civitarese, Phys. Rep. **300**, 123 (1998).

[2] M. Aunola and J. Suhonen, Nucl. Phys. **A602**, 133 (1996).

[3] A. S. Barabash and R. R. Saakyan, Phys. At. Nucl. **59**, 179 (1996).

[4] M. Hirsch, K. Muto, T. Oda, and H. V. Klapdor-Kleingrothaus, Z. Phys. A **53**, 2136 (1994).

[5] M. J. Inghram and J. H. Reinolds, Phys. Rev. **78**, 822 (1950).

[6] N. Takaoka and K. Ogata, Z. Naturforsch. A **21**, 84 (1966).

[7] N. Takaoka, J. Okano, and O. Koreichi, Adv. Mass Spectrom. **4**, 943 (1968).

[8] N. Takaoka, Y. Motomura, and K. Nagao, J. Mass Spectrom. Soc. Jpn. **44**, 63 (1996).

[9] N. Takaoka, Y. Motomura, and K. Nagao, Phys. Rev. C **53**, 1557 (1996).

[10] T. Kirsten, W. Gentner, and O. A. Schaeffer, Z. Phys. **202**, 273 (1967).

[11] T. Kirsten, O. A. Schaeffer, E. Norton, and R. W. Stoenner, Phys. Rev. Lett. **20**, 1300 (1968).

[12] T. Kirsten, H. Richter, and E. K. Jessberger, Z. Phys. C **16**, 189 (1983).

[13] W. J. Lin, O. K. Manuel, G. Cummings, D. Krstic, and R. I. Thorpe, Nucl. Phys. **A481**, 477 (1988).

[14] J. F. Richardson, O. K. Manuel, and B. Sinha, Nucl. Phys. **A453**, 26 (1986).

[15] J. T. Lee and O. K. Manuel, Nucl. Phys. **A529**, 29 (1991).

[16] O. K. Manuel, J. Phys. G **17**, 221 (1991).

[17] T. Bernatowicz, J. Brannon, R. H. Brazzle, R. Cowsik, C. M. Hohenberg, and F. Podosek, Phys. Rev. Lett. **69**, 2341 (1992).

[18] T. Bernatowicz, J. Brannon, R. H. Brazzle, R. Cowsik, C. M. Hohenberg, and F. Podosek, Phys. Rev. C **47**, 806 (1993).

[19] S. R. Elliott, A. A. Hahn, and M. K. Moe, Phys. Rev. Lett. **59**, 2020 (1987).

[20] B. Srinivasan, Earth Planet. Sci. Lett. **31**, 129 (1976).

[21] B. Li, J. T. Lee, and O. K. Manuel, Earth Planet. Sci. Lett. **123**, 71 (1994).

[22] B. A. Lubchenko and V. M. Patc, Razved. Okhr. Nedr **12**, 24 (1967).

[23] V. G. Krivovichev, Zap. Vses. Mineral. O-va. **100**, 462 (1971).

[24] A. I. Fridman, A. I. Remisova, G. I. Voitov, and L. F. Cherevichnaya, Dokl. Akad. Nauk SSSR **233**, 470 (1977).

[25] Yu. M. Dymkov, V. V. Kazantsev, and V. A. Lubchenko, in *Mestorozhdenia Urana: Zonal'nost' Paragenezisy*, edited by D. Ya. Surazhskii (Atomizdat, Moscow, 1970).

[26] C. M. Hohenberg, Rev. Sci. Instrum. **51**, 1075 (1980).

[27] A. P. Meshik, Ph.D. thesis, Vernadsky Institute, 1988.

[28] B. G. Young and H. G. Thode, Can. J. Phys. **38**, 1 (1960).

[29] S. Valkiers, Y. Aregbe, P. D. P. Taylor, and P. De Bievre, Int. J. Mass Spectrom. Ion Processes **173**, 55 (1998).

[30] J. Eikenberg, P. Signer, and R. Wieler, Geochim. Cosmochim. Acta **57**, 1053 (1993).

[31] R. A. Ragettli and E. H. Hebeda, Earth Planet. Sci. Lett. **128**, 653 (1994).

[32] A. P. Meshik, K. Kehm, and C. M. Hohenberg, Geochim. Cosmochim. Acta **64**, 1651 (2000).